10th ANKARA INTERNATIONAL AEROSPACE CONFERENCE
18-20 September 2019 - METU, Ankara TURKEY

**AIAC-2019-203**

# ACOUSTIC CHARACTERIZATION OF A ROCKET COMBUSTION CHAMBER

Yusuf ÖZYÖRÜK*
Middle East Technical University
Ankara, Turkey

Gizem DEMİREL†
TOBB University
Ankara, Turkey

## ABSTRACT

*Acoustic fluctuations coupled with unsteady combustion with similar phase lead to thermoacoustic instabilities in rocket combustion chambers. If not controlled these oscillations may grow above critical levels leading to serious vibrations and even failure of the engine. Design and evaluation of a combustion chamber to this respect require knowledge of its acoustic modal structure and resonant frequencies. This paper discusses a Helmholtz equation solver for obtaining such information, with full reflective conditions at the converging-diverging nozzle throat and without convective effects. The resonant frequencies with flow effects are determined through time-domain Euler computations of full, open throat configuration with random inlet disturbances and a subsequent Fast Fourier Transform process applied to collected unsteady pressure data. An example application is made to a generic geometry. Despite the differences in the nozzle throat treatment, both solution approaches were expected to produce similar frequencies for the resolved first few longitudinal modes, as a consequence of strong natural reflections from the converging part of the nozzle in the Euler simulations. However, such frequency similarity was not obtained. The reason is attributed mainly to the different inlet boundary condition treatments of the two approaches.*

## INTRODUCTION

Combustion instability is a serious concern in rocket development [Harrje and Reardon, 1972; Culick and Yang, 1995; Culick, 1998]. Because of the partially confined nature of combustion chamber volume, it has an inherent acoustic environment to which the heat release mechanisms may couple such that the rate at which unsteady energy addition by combustion is larger than the rate of damping through the flow's destruction mechanisms, boundaries, and the nozzle. Coupling occurring this way leads to combustion instabilities. Energy gain or damping point was put in a simple mathematical perspective by Rayleigh [1945] as

$$R = \int_T \int_{\mathcal{V}} p'(\vec{x},t) q'(\vec{x},t)\, d\mathcal{V}\, dt \tag{1}$$

where $p'$ describes the pressure perturbation, and $q'$ the unsteady heat release. Once the integral $R$ is positive, thermoacoustic instability will be observed. This is called the Rayleigh criteria [Culick

*Professor, Department of Aerospace Engineering, E-mail: yusuf.ozyoruk@ae.metu.edu.tr
†Graduate Student, Department of Mechanical Engineering, E-mail: gizem.demirel13@gmail.com

and Yang, 1995]. This simple mathematical form may be interpreted as follows. When the phase difference at a point between a pressure perturbation and heat release perturbation is less than that corresponding to one quarter of their period, that point in the chamber will contribute positively to the growth of perturbations.

Whether a positive contribution will exist or not depends on many complex, distributed, physical actions in a combustion chamber. For example, in liquid propellant rocket engine chambers, acoustic waves influence the injection of the propellants. Formation of droplets, their mixing and evaporation may change character under strong oscillations, especially by those high-frequency transverse waves near the injector surface [Vingert *et al.*, 1995; Popov *et al.*, 2015]. In solid propellant rocket engines vortices may shed from inhibitors or along the surface of the propellant [French *et al.*, 2017], and gas generation from the reacting surface of the solid propellant may be quite unsteady [Flandro and Majdalani, 2003; Saha and Chakraborty, 2017], all due to coupling with the acoustic field in the chamber. Response of individual mechanisms to an oscillation component may result in time delays which may be within one quarter of oscillation period at the point of heat release, contributing positively to the unsteadiness of it.

Understanding whether all these will happen in a given design requires detailed knowledge of the chamber's acoustic field [Flandro and Majdalani, 2003; Nicoud *et al.*, 2007; Cengiz and Özyörük, 2013; Urbano *et al.*, 2016; Schmitt *el al.*, 2017], and response of the various mechanisms [Popov *et al.*, 2015; Gruhlke *et al.*, 2016] to it. It is, therefore, the purpose of the present work to develop a framework to study thermoacoustic instabilities in a combustion chamber. However, prior knowledge on acoustics character of the chamber is needed as input to the algorithms to study the instability phenomena. This paper deals with acoustic characterization of a generic chamber. Acoustic analysis is performed using two different approaches. Acoustic modal structure in the whole combustion chamber is obtained using a Helmholtz equation solver developed as part of the framework. Helmholtz solutions are often carried out assuming strong reflections occur from the throat area (see, for example, Nicoud *et al.* [2007]; Urbano *et al.* [2016]). This is the assumption made also in this paper when a frequency domain solution is sought. However, some acoustic energy escapes through the nozzle, which modifies the chamber frequencies to some degree. Therefore, resonant frequencies in the full chamber plus nozzle configuration with flow are determined by a time-domain approach. These are described below.

## METHODOLOGY

### Frequency domain analysis

Helmholtz equation: Assuming thermoacoustic instability starts with small perturbations, at the onset one may write flow state is composed of a mean plus a perturbation :

$$\vec{q}(\vec{x},t) = \vec{q}_0(\vec{x}) + \vec{q'}(\vec{x},t) \tag{2}$$

where subscript 0 signifies a mean, and prime sign signifies perturbation. Also, viscous effects are negligible. Substituting this decomposition into the mass and momentum conservations, and neglecting 2nd and higher-order terms in fluctuations, one obtains the linear mass and momentum equations. By differentiating the former with respect to time and taking the divergence of the latter, and subtracting the resultant equations from each other, a second-order linear partial differential equation governing the fluctuations is obtained. Since a hot environment exists within the chamber and fluid velocities are negligibly small compared to sound speed $c_0(\vec{x})$ (Mach number is small), further simplification leads to

$$\frac{1}{\bar{c}_0^2}\frac{\partial^2 p'(\vec{x},t)}{\partial t^2} + \left(\frac{c_0(\vec{x})}{\bar{c}_0}\right)^2 \rho_0(\vec{x})\nabla\cdot\left(\frac{\nabla p'(\vec{x},t)}{\rho_0(\vec{x})}\right) = 0 \tag{3}$$

where $\bar{c}_0$ is reference sound speed (e.g. volume averaged one), and $c_0(\vec{x})$ is the local sound speed. It is clear the latter sound speed is $\vec{x}$-dependent. This is in general due to combustion resulting in non-homogeneous mean temperature and density in the chamber.

Heat sources may also be included on the right-hand side of this equation. This can be done by applying the same procedure to the couple of the linear momentum and energy equations. In this case, the wave equation reads,

$$\frac{1}{\bar{c}_0^2}\frac{\partial^2 p'(\vec{x},t)}{\partial t^2} + \left(\frac{c_0(\vec{x})}{\bar{c}_0}\right)^2 \rho_0(\vec{x})\nabla\cdot\left(\frac{\nabla p'(\vec{x},t)}{\rho_0(\vec{x})}\right) = -\frac{1}{\gamma-1}\frac{\partial q'(\vec{x},t)}{\partial t} \tag{4}$$

where $\gamma$ is the ratio of specific heats, and $q'$ on the right hand side represents the unsteady heat addition.

Acoustic pressure may be expanded into sinusoidal components of varying amplitudes and frequencies. Then, each component must satisfy the above equation with the same boundary conditions. These points may be taken into account automatically by Fourier transform of the wave equation and the boundary conditions. Then, the wave equation in frequency domain reads

$$\frac{\omega^2}{\bar{c}_0^2}\hat{p}(\vec{x}) + \left(\frac{c_0(\vec{x})}{\bar{c}_0}\right)^2 \rho_0(\vec{x})\nabla\cdot\left(\frac{\nabla\hat{p}(\vec{x})}{\rho_0(\vec{x})}\right) = -\frac{i\omega}{\gamma-1}\hat{q}(\vec{x}) \tag{5}$$

where $\omega$ is circular frequency, $\hat{p}$ and $\hat{q}$ are the Fourier transforms of the pressure and heat perturbations. This equation is called the Helmholtz equation.

Boundary conditions: Chamber boundaries are assumed rigid, including the throat section. Since the normal component of particle velocity at such boundaries vanishes, the boundary condition is

$$(\hat{n}\cdot\nabla\hat{p})|_{\text{wall}} = 0 \tag{6}$$

Discretization: The homogeneous form of the wave equation is discretized using finite volume approach. The physical domain is subdivided into small elements. The elements may consist of a blend of tetrahedra, pyramid, prism, wedges, and hexahedra.

The evaluation of the terms of the wave equation on the mesh requires gradients at the element faces. They are obtained by averaging the cell-based gradients of the cells sharing the faces. The cell-based gradients are computed using the Green-Gauss approach. For a cell indexed by $j$, it reads :

$$\nabla\hat{p}_j = \frac{1}{\mathcal{V}_j}\sum_f^{N_{f_j}} \hat{p}_{j,f}\Delta\vec{\mathcal{S}}_{j,f} \tag{7}$$

where $\mathcal{V}_j$ is the $j$-th cell volume, $\Delta\vec{S}_{j,f}$ is the $f$-th face area vector of cell $j$. Then, the pressure gradient on a face is obtained from gradient information from its left and right owners $L$ and $R$ by

$$\nabla\hat{p}_{LR} = \overline{\nabla\hat{p}_{LR}} + \left[\frac{\hat{p}_R-\hat{p}_L}{|\vec{r}_{LR}|} - \overline{\nabla\hat{p}_{LR}}\cdot\hat{r}_{LR}\right]\hat{r}_{LR} \tag{8}$$

where

$$\overline{\nabla\hat{p}_{LR}} \;= \tfrac{1}{2}\Big(\nabla\hat{p}_L + \nabla\hat{p}_R\Big), \quad \vec{r}_{LR} \;= \vec{r}_R - \vec{r}_L, \quad \hat{r}_{LR} = \frac{\vec{r}_{LR}}{|\vec{r}_{LR}|} \tag{9}$$

Hence, applying this type of discretization to all elements we get for the homogeneous Helmholtz equation,

$$k^2\hat{p}_j + \frac{1}{\mathcal{V}_j}\left(\frac{c_0}{\bar{c}_0}\right)_j^2 \rho_{0,j}\sum_f^{N_{f_j}}\left(\frac{\nabla\hat{p}}{\rho_0}\cdot\Delta\vec{\mathcal{S}}\right)_{j,f} = 0 \tag{10}$$

or alternatively using matrix-vector operation, the whole system of algebraic equations are written as

$$[A]\,\{\hat{p}\} = -k^2\{\hat{p}\} = \lambda\{\hat{p}\}. \tag{11}$$

Solution: This set of linear equations forms an eigenvalue problem. The eigenvalues of the system, $\lambda = -k^2$, which form the resonant frequencies in the chamber, and consequently the eigenfunctions which form the chamber acoustic modal structures are determined using the freely available ARPACK Arnoldi algorithm package [Lehoucq, 1998].

### Time domain approach

As aforementioned a frequency domain analysis is done assuming full reflections from the nozzle throat as well as no flow exist. However, due to acoustic leakage through the nozzle, which is called nozzle damping, modifications to the modal structure and frequencies should be expected to some degree. Incorporating these effects in the Helmholtz equation solver results in complications. On the other hand, one may quickly observe the effects of the nozzle flow on the frequencies by solving either linearized Euler equations or full non-linear Euler equations in time domain. This is done by obtaining a steady flow first, and then integrating the time-dependent Euler equations with perturbations at a broad range of random frequencies to the inlet total pressure and total temperature values of the chamber. After the initial transients due to switching from steady to unsteady computations are gone, pressure data at various positions in the chamber are collected. The data are then processed using Fast Fourier Transform (FFT) which gives the spectral distribution for the chamber sound field.

The applied inlet total pressure and temperature distortions are given as follows:

$$\vec{q}_{\text{in}}(\vec{x}_0, t) = \vec{q}_{\text{in},0}(\vec{x}_0)\left[1 + \epsilon \sum_{j=1}^{N_f} \cos(2\pi f_j t + \phi_j)\right] \tag{12}$$

where $\vec{q}_{\text{in},0}(\vec{x}_0)$ is the vector of mean total pressure and total temperature at the inlet, $\vec{q}_{\text{in}}(\vec{x}_0)$ is the instantaneous counterpart, $\epsilon$ is perturbation ratio, taken as $0.05$ in this paper, $f_j$ and $\phi_j$ are the $j$-th random frequency and phase, respectively.

## RESULTS AND DISCUSSION

### Frequency domain solutions

The Helmholtz solver is tested in this section. The first test configuration is a simple rectangular volume with dimensions of $L = 1$ m, and $H = 0.25$ m with rigid walls. Sound speed in the volume is 340 m/s. A hybrid mesh with triangular and quadrilateral elements is used for the solution. The analytical modal solution with unit amplitude and the corresponding resonant frequencies are given for the volume as

$$\begin{aligned} \hat{p}(x, y) &= \cos\left(\frac{m\pi x}{L}\right)\cos\left(\frac{n\pi y}{H}\right), \quad m = 0, 1, 2, \ldots \ ; \ n = 0, 1, 2, \ldots \\ f_{m,n} &= \frac{c_0}{2\pi}\sqrt{\left(\frac{m\pi}{L}\right)^2 + \left(\frac{n\pi}{H}\right)^2} \end{aligned} \tag{13}$$

The mesh and the computed $(m, n) = (4, 1)$ mode are shown in Figure 1. A comparison of the particular frequencies for several modes with the analytically obtained frequencies is made in Table 1. It is evident that the Helmholtz solver captured the frequencies of the indicated modes very accurately.

The second case involves a typical combustion chamber modal analysis. The geometry is treated as axisymmetric, and hence the Helmholtz equation is solved in cylindrical $(x, r)$ coordinates with a modal decomposition in the azimuthal direction $\theta$ given by

$$\hat{p}(x, r, \theta) = \tilde{p}(x, r)e^{-im\theta} \tag{14}$$

This way the 2nd-order spatial derivative in the $\theta$ direction is transformed into an analytically obtained source, for a specified azimuthal mode order of $m$. The chamber is terminated at the nozzle throat with a hypothetically full reflective response. The computed acoustic mode structures for azimuthal

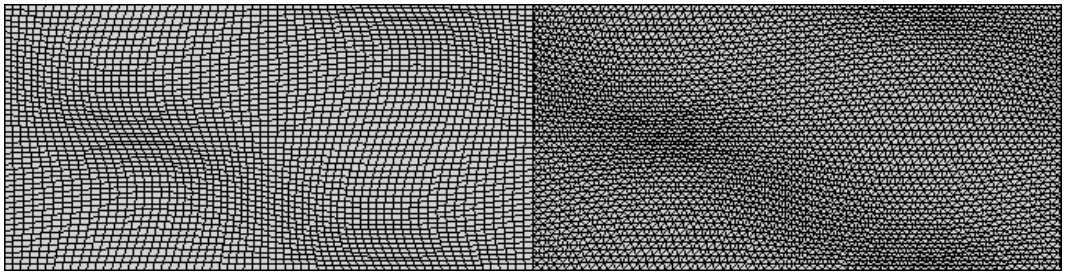

(a) hybrid mesh

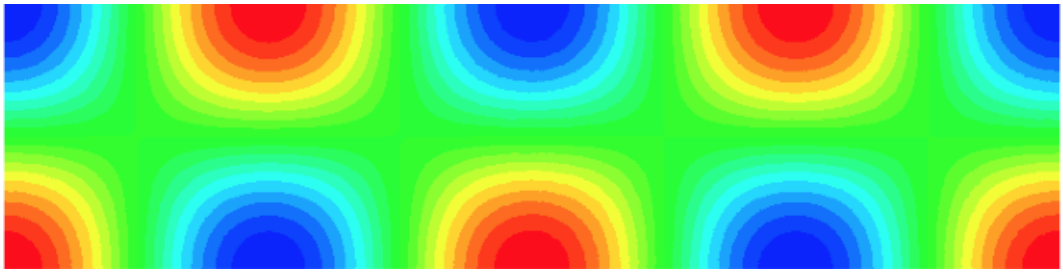

(b) $(m, n) = (4, 1)$ mode

Figure 1: Rectangular closed volume mesh and $(4, 1)$ mode structure.

Table 1: Modal frequencies in rectangular volume with rigid walls.

| $(m,n)\downarrow,\ f\rightarrow$ | analytic | numerical |
|---|---|---|
| (1,0) | 85.00 | 85.00 |
| (2,0) | 170.00 | 170.00 |
| (3,0) | 255.00 | 255.00 |
| (1,1) | 350.46 | 350.36 |
| (2,1) | 380.13 | 380.03 |
| (3,1) | 425.00 | 424.89 |
| (4,1) | 480.83 | 480.62 |

mode orders of $m = 0, 1, 2$, and 3 are shown in Figure 2. Higher-order modes appear in the chamber at higher frequencies as expected.

### Time domain solutions

Resonant frequencies in a combustion chamber are found by solving the flow equations in a time-dependent manner with arbitrary forcing of the inlet conditions with small deviations from the mean states, and a subsequent FFT applied to the collected data. Figure 3 shows the computational mesh used for the Euler calculations, and the computed mean Mach number distribution. Beginning from the steady flow with the inlet conditions at a $x = x_0$ constant plane perturbed randomly, unsteady computations capture the acoustic phenomena in the chamber. FFT applied to the data collected at a point in the chamber yielded the frequency responses shown in Figure 4. It is evident there are significantly higher sound pressure levels at some frequencies. A 20 dB higher sound pressure level (SPL) at a frequency shows one order of magnitude higher pressure perturbation. Hence, very high SPL levels correspond to the sustained acoustic fluctuations in the chamber, and the corresponding frequencies are the resonant frequencies.

### Evaluation of the results

Longitudinal modes ($m = 0$, plane waves) occur at lower frequencies than transverse (radial) or tangential ($m \neq 0$) modes. The frequency domain calculations with a closed chamber (i.e. hypothetically full reflective throat section) indicated the first longitudinal mode occurs at 1376.6 Hz (Figure 2a),

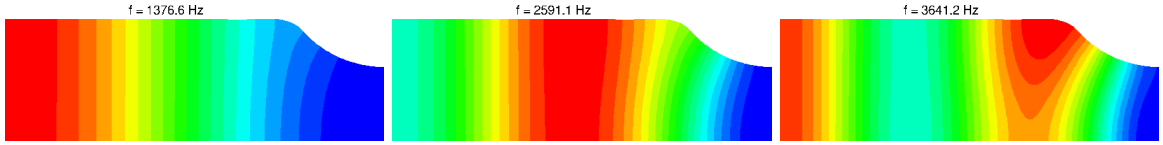


(a) $m = 0$ modes, @ 1376.6, 2591.1, 3641.2 Hz

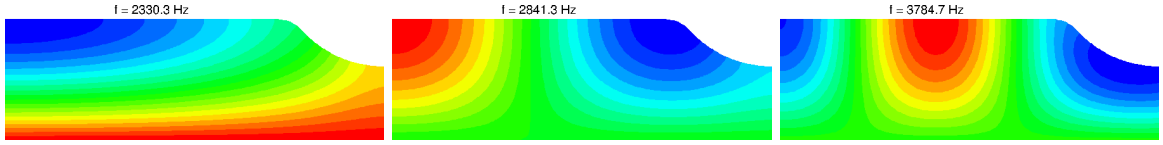


(b) $m = 1$ modes, @ 2330.3, 2841.3, 3784.7 Hz

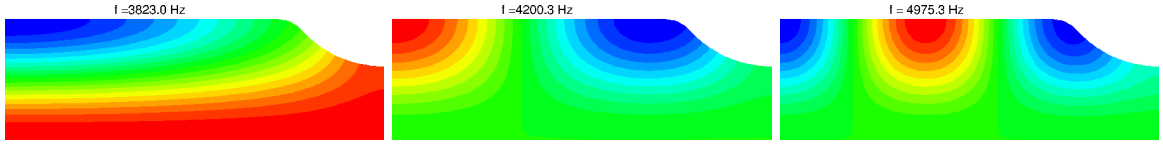


(c) $m = 2$ modes, @ 3823.0, 4200.3, 4975.3 Hz

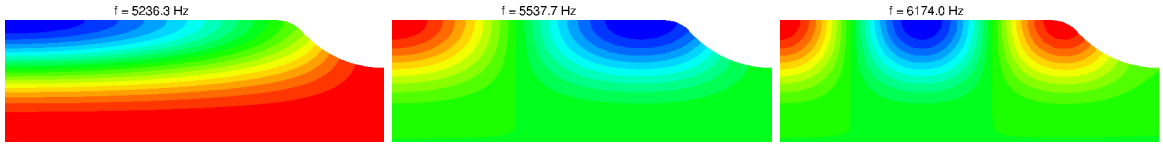


(d) $m = 3$ modes, @ 5236.3, 5537.7, 6174.0 Hz

Figure 2: Acoustic mode structures in generic combustion chamber.

but in reality the open throat which is chocked at the assumed chamber stagnation conditions causes somewhat a different boundary condition there. If the Euler computations had been somehow done with full reflective upstream inlet conditions, one could have expected a frequency not very far from that found by the Helmholtz solver, mainly due to expectation of strong reflections from the convergent part of the nozzle. However, the time-domain calculation predicted a frequency which is almost half (Figure 4a) of that given by the Helmholtz solution. Having the first significant peak in the FFT results of the time-domain solution at 744.6 Hz indicates the simulated inlet boundary condition by the Euler solver in fact differs from a rigid wall condition.

The frequencies of the other acoustic modes dominant in the actual situation (open throat) appear to be about 2.35 kHz (Figure 4b), 3.2 kHz (Figure 4b), and so on. The higher frequencies pertain to azimuthal and radial modes.

In order to treat the inlet and throat conditions more accurately in frequency domain, the local impedance conditions there must be known and implemented in the Helmholtz solver. However, the usage of a non-rigid boundary condition complicates the eigenvalue problem, which is a subject of current code development. Time-domain approach has no such a difficulty for the throat section, but the perturbed inlet conditions must be able to bring the flow and at the same time represent the actual impedance there.

## CONCLUSIONS

A framework for studying rocket engine combustion instabilities is being developed. The algorithms of this framework require the acoustical modal structures in the chamber a priori. A Helmholtz equation solver has been developed using finite volume algorithm. The discretized equations form an eigenvalue problem which is solved by the ARPACK package for the resonant frequencies. The corresponding modal structures are also found using the same eigensolver. The resonant frequencies may also be determined using time-domain analysis approach in which the chamber inlet conditions are deviated from their mean values by disturbances within a spectrum of random frequencies. The approaches have

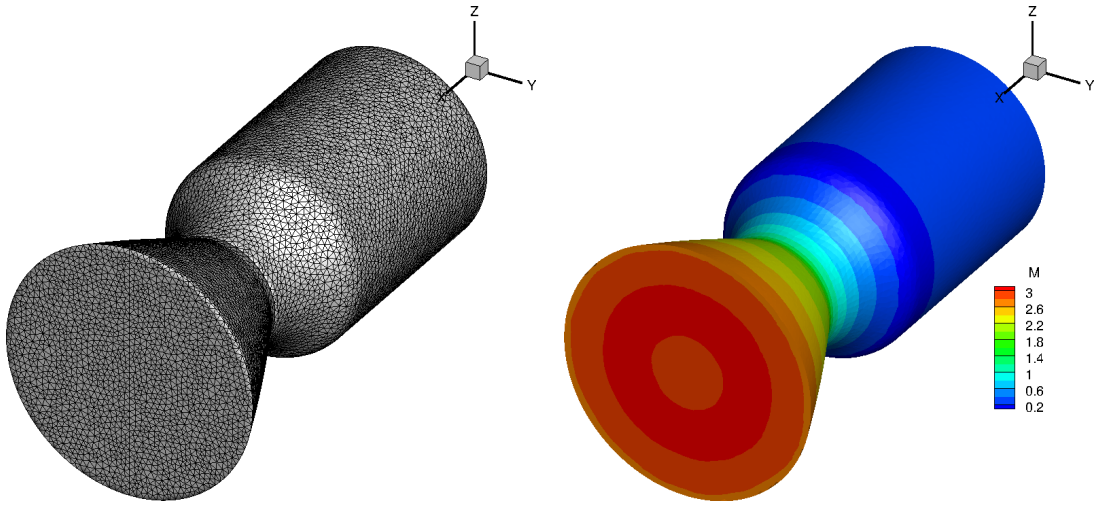


(a) mesh (b) Mach

Figure 3: Steady flow solution for the generic combustion chamber.

been applied to a generic combustion chamber geometry. Despite the differences in the nozzle throat treatment, both solution approaches were expected to produce similar frequencies for the resolved first few longitudinal modes, as a consequence of strong natural reflections from the converging part of the nozzle in the Euler simulations. However, such frequency similarity was not obtained. The reason is attributed mainly to the different inlet boundary condition treatments of the two approaches.

## References

Cengiz, K. and Özyörük, Y. (2013) *A Helmholtz-type numerical simulation of thermo-acoustic instabilities in a 3-D Rijke tube*, AIAA Paper 2013-4060, 49th AIAA/ASME/SAE/ASEE Joint Propulsion Conference and Exhibit, San Jose, CA, USA.

Culick, F. E. C. (1998) *Combustion instabilities in liquid-fueled propulsion systems - an overview*, AGARD Conference Proceedings, no. 450.

Culick, F. E. C. and Yang, V. (1995) *Overview of combustion instabilities in liquid-propellant rocket engines*, Liquid Rocket Engine Combustion Instability, Progress in Astronautics and Aeronautics, No. 169, AIAA.

Flandro, G. A. and Majdalani, J. (2003) *Thermoacoustic Instability in Rockets*, AIAA Journal, vol. 41, no. 3, pp. 485–497.

French, A. and Panelli, M. and Di Lorenzo, G. and Schettino, A. and Paglia, F. (2017) *Combustion instability and pressure oscillation numerical simulation in a solid rocket motor*, 53rd AIAA/ASME/ASEE Joint Propulsion Conference, 10-12th July, Atlanta, Georgia.

Gruhlke, P. and Mahiques, E. I. and Meisl, J. and Kaufmann, P. and Kempf, A. and Kok, J. B. W. (2016) *The acoustic response of reacting sprays in cross-flow models to forced excitations*, 23rd International Congress on Sound and Vibration, Athens, Greece.

Harrje, D. J. and Reardon, F. H. (1972) *Liquid propellant rocket instability*, NASA SP-194.

Lehoucq, R. B. (1998) *ARPACK User's Guide Solution of Large-scale Eigenvalue Problems with Implicitly Restarted Arnoldi Methods* , SIAM, 3600 Market Street, Floor 6, Philadelphia, PA.

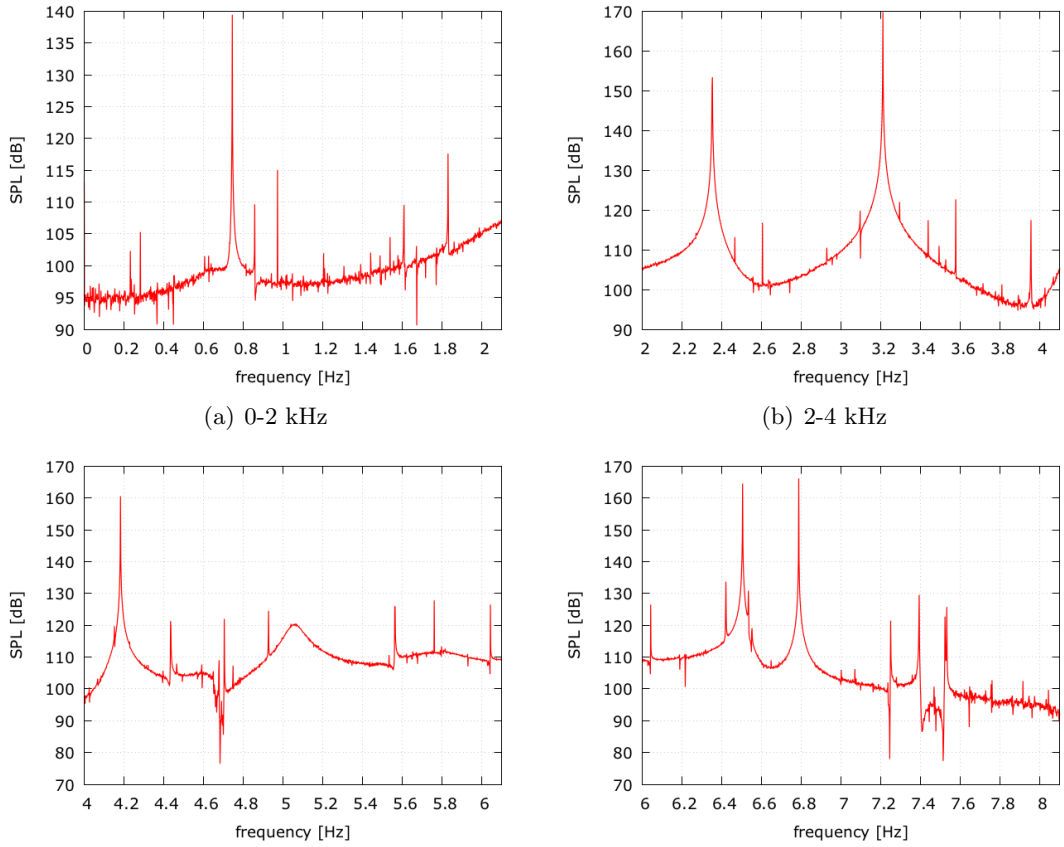


(a) 0-2 kHz (b) 2-4 kHz

(c) 4-6 kHz (d) 6-8 kHz

Figure 4: Acoustically resonant frequencies in generic combustion chamber.

Nicoud, F. and Benoit, L. and Sensiau, C. and Poinsot, T. (2007) *Acoustic modes in Combustors with Complex Impedances and Multidimensional Active Flames*, AIAA Journal, vol. 45, no. 2, pp. 426–441.

Popov, P. and Sirignano, W. A. and Sideris, A. (2015) *Propellant injector influence on liquid-propellant rocket engine instability*, Journal of Propulsion and Power, vol. 31, no. 1, pp. 320–331.

Rayleigh, L. (1945) *The Theory of Sound, Volume Two*, Dover Publications, New York.

Saha, S. and Chakraborty, D. (2017) *Computational fluid dynamics simulation of combustion instability in solid rocket motor : implementation of pressure coupled response function*, Defence Sciences Journal, vol. 66, pp. 216-221.

Schmitt, T. and Staffelbach, G. and Ducruix, S. and Groning, S. and Hardi, J. and Oschwald, M. (2017), *Large-Eddy Simulations of a sub-scale liquid propellant combustor: influence of fuel injection temperature on thermo-acoustic stability*, 7th European Conference for Aeronautics and Aerospace Sciences, EUCASS.

Urbano, A. and Selle, L. and Staffelbach, G. and Cuenot, B. and Schmitt, T. and Ducruix, S. and Candel, S. (2016), *Exploration of combustion instability triggering using Large Eddy Simulation of a multiple injector liquid rocket engine*, Combustion and Flame, vol. 169, 129–140.

Vingert, L. and Gicquel, P. and Lourme, D. and Menoret, L. (1995) *Coaxial Injector Atomization*, Liquid Rocket Engine Combustion Instability, Progress in Astronautics and Aeronautics, No. 169, AIAA.